

Structure formation via a late-time vacuum phase transition




We explore how a vacuum phase transition in the post-recombination era may provide a solution to a potentially troublesome cosmological problem

Amol V. Patwardhan



University of California, San Diego
Center for Astrophysics and Space Sciences

August 27, 2013

References I

-  Amol V. Patwardhan and George M. Fuller
Structure formation via a late-time vacuum phase transition
To be submitted to PRD
-  Joel R. Primack and Mark A. Sher
Photon mass at low temperature?
Nature 288 (18): 680–681, 1980.
-  Ira Wasserman
Late Phase Transitions and the Spontaneous Generation of
Cosmological Density Perturbations
Phys. Rev. Lett. 57 (17): 2234–2236, 1986.

References II

-  **George M. Fuller and David N. Schramm**
Late-phase-transition-induced fluctuations in the cosmic neutrino distribution and the formation of structure in the Universe
Phys. Rev. D 45 (8): 2595–2600, 1992.
-  **Craig J. Hogan**
Nucleation of Cosmological Phase Transitions
Physics Letters B 133 (3-4): 172–176, 1983.

Outline

- 1 Big Black Holes and Late phase transitions
- 2 Sweeping up vacuum energy, à la Wasserman
- 3 Constraints
- 4 Conclusion

Big Black Holes

- Observational evidence points to the existence of big black holes (10^9 – $10^{10} M_{\odot}$) at high redshifts ($z \sim 5$ – 7),

doi:10.1038/nature10159

A luminous quasar at a redshift of $z = 7.085$

Daniel J. Mortlock¹, Stephen J. Warren¹, Bram P. Venemans², Mitesh Patel¹, Paul C. Hewett¹, Richard G. McMahon³, Chris Simpson⁴, Tom Theuns^{5,6}, Eduardo A. González-Solares³, Andy Adamson⁷, Simon Dye⁸, Nigel C. Hambly⁹, Paul Hirst¹⁰, Mike J. Irwin³, Ernst Kuiper¹¹, Andy Lawrence⁹ & Huub J. A. Röttgering¹¹

The intergalactic medium was not completely reionized until approximately a billion years after the Big Bang, as revealed¹ by observations of quasars with redshifts of less than 6.5. It has been difficult to probe to higher redshifts, however, because quasars have historically been identified^{2–4} in optical surveys, which are insensitive to sources at redshifts exceeding 6.5. Here we report observations of a quasar (ULAS J112001.48+064124.3) at a redshift of 7.085, which is 0.77 billion years after the Big Bang. ULAS J1120+0641 has a luminosity of $6.3 \times 10^{13} L_{\odot}$ and hosts a black hole with a mass of $2 \times 10^9 M_{\odot}$ (where L_{\odot} and M_{\odot} are the luminosity and mass of the Sun). The measured radius of the ionized near zone around ULAS J1120+0641 is 1.9 megaparsecs, a factor of three smaller than is typical for quasars at redshifts between 6.0 and 6.4. The near-zone transmission profile is consistent with a Ly α damping wing⁵, suggesting that the neutral fraction of the intergalactic medium in front of ULAS J1120+0641 exceeded 0.1.

photometry from UKIDSS, the Sloan Digital Sky Survey⁷ (SDSS) and follow-up observations on UKIRT and the Liverpool Telescope (listed in Fig. 1) was consistent⁸ with a quasar of redshift $z \gtrsim 6.5$. Hence, a spectrum was obtained using the Gemini Multi-Object Spectrograph on the Gemini North Telescope on the night beginning 27 November 2010. The absence of significant emission blueward of a sharp break at $\lambda = 0.98 \mu\text{m}$ confirmed ULAS J1120+0641 as a quasar with a preliminary redshift of $z = 7.08$. Assuming a fiducial flat cosmological model⁹ (that is, cosmological density parameters $\Omega_m = 0.26$, $\Omega_b = 0.024$, $\Omega_{\Lambda} = 0.74$ and current value of the Hubble parameter $H_0 = 72 \text{ km s}^{-1} \text{ Mpc}^{-1}$), ULAS J1120+0641 is seen as it was 12.9 billion years (Gyr) ago, when the Universe was 0.77 Gyr old. Although three sources have been spectroscopically confirmed to have even higher redshifts, two are faint $J_{AB} \gtrsim 26$ galaxies^{10,11} and the other is a γ -ray burst, which has since faded¹². Indeed, it has not been possible to obtain high signal-to-noise ratio spectroscopy of any sources beyond the most dis-

Big Black Holes

- Observational evidence points to the existence of big black holes (10^9 – $10^{10} M_{\odot}$) at high redshifts ($z \sim 5$ – 7),
- ~ 1 Gyr since the beginning of time

doi:10.1038/nature10159

A luminous quasar at a redshift of $z = 7.085$

Daniel J. Mortlock¹, Stephen J. Warren¹, Bram P. Venemans², Mitesh Patel¹, Paul C. Hewett¹, Richard G. McMahon³, Chris Simpson⁴, Tom Theuns^{5,6}, Eduardo A. González-Solares³, Andy Adamson⁷, Simon Dye⁸, Nigel C. Hambly⁹, Paul Hirst¹⁰, Mike J. Irwin³, Ernst Kuiper¹¹, Andy Lawrence⁹ & Huub J. A. Röttgering¹¹

The intergalactic medium was not completely reionized until approximately a billion years after the Big Bang, as revealed¹ by observations of quasars with redshifts of less than 6.5. It has been difficult to probe to higher redshifts, however, because quasars have historically been identified^{2–4} in optical surveys, which are insensitive to sources at redshifts exceeding 6.5. Here we report observations of a quasar (ULAS J112001.48+064124.3) at a redshift of 7.085, which is 0.77 billion years after the Big Bang. ULAS J1120+0641 has a luminosity of $6.3 \times 10^{13} L_{\odot}$ and hosts a black hole with a mass of $2 \times 10^9 M_{\odot}$ (where L_{\odot} and M_{\odot} are the luminosity and mass of the Sun). The measured radius of the ionized near zone around ULAS J1120+0641 is 1.9 megaparsecs, a factor of three smaller than is typical for quasars at redshifts between 6.0 and 6.4. The near-zone transmission profile is consistent with a Ly α damping wing⁵, suggesting that the neutral fraction of the intergalactic medium in front of ULAS J1120+0641 exceeded 0.1.

photometry from UKIDSS, the Sloan Digital Sky Survey⁷ (SDSS) and follow-up observations on UKIRT and the Liverpool Telescope (listed in Fig. 1) was consistent⁸ with a quasar of redshift $z \gtrsim 6.5$. Hence, a spectrum was obtained using the Gemini Multi-Object Spectrograph on the Gemini North Telescope on the night beginning 27 November 2010. The absence of significant emission blueward of a sharp break at $\lambda = 0.98 \mu\text{m}$ confirmed ULAS J1120+0641 as a quasar with a preliminary redshift of $z = 7.08$. Assuming a fiducial flat cosmological model⁹ (that is, cosmological density parameters $\Omega_m = 0.26$, $\Omega_b = 0.024$, $\Omega_{\Lambda} = 0.74$ and current value of the Hubble parameter $H_0 = 72 \text{ km s}^{-1} \text{ Mpc}^{-1}$), ULAS J1120+0641 is seen as it was 12.9 billion years (Gyr) ago, when the Universe was 0.77 Gyr old. Although three sources have been spectroscopically confirmed to have even higher redshifts, two are faint $J_{AB} \gtrsim 26$ galaxies^{10,11} and the other is a γ -ray burst, which has since faded¹². Indeed, it has not been possible to obtain high signal-to-noise ratio spectroscopy of any sources beyond the most dis-

Late Phase Transitions

- Concept introduced by Primack and Sher [2] as a means of giving photons mass at low temperature

Late Phase Transitions

- Concept introduced by Primack and Sher [2] as a means of giving photons mass at low temperature
- Idea caught on as a mechanism to generate density fluctuations in the early universe [3, 4]

Late Phase Transitions

- Concept introduced by Primack and Sher [2] as a means of giving photons mass at low temperature
- Idea caught on as a mechanism to generate density fluctuations in the early universe [3, 4]
- Different ways of generating fluctuations: via slow roll dynamics, **bubble nucleation**, topological defects etc.

Why Late?

- In standard cosmology, density fluctuations produced prior to photon decoupling seed the growth of structure at late times

Why Late?

- In standard cosmology, density fluctuations produced prior to photon decoupling seed the growth of structure at late times
- Highly evolved structures at large redshifts difficult to explain, given the high CMB isotropy

Why Late?

- In standard cosmology, density fluctuations produced prior to photon decoupling seed the growth of structure at late times
- Highly evolved structures at large redshifts difficult to explain, given the high CMB isotropy
- Density perturbations generated prior to recombination experience damping via radiation diffusion

Why Late?

- In standard cosmology, density fluctuations produced prior to photon decoupling seed the growth of structure at late times
- Highly evolved structures at large redshifts difficult to explain, given the high CMB isotropy
- Density perturbations generated prior to recombination experience damping via radiation diffusion
- Post-recombination-phase-transition-induced perturbations in the CMB can be well within observational bounds

Why Late?

- In standard cosmology, density fluctuations produced prior to photon decoupling seed the growth of structure at late times
- Highly evolved structures at large redshifts difficult to explain, given the high CMB isotropy
- Density perturbations generated prior to recombination experience damping via radiation diffusion
- Post-recombination-phase-transition-induced perturbations in the CMB can be well within observational bounds
 - We're most interested in $T_c \sim 0.01\text{--}0.1$ eV

Outline

- 1 Big Black Holes and Late phase transitions
- 2 Sweeping up vacuum energy, à la Wasserman
- 3 Constraints
- 4 Conclusion

Phase transition - dynamics

- Bubbles begin nucleating at some post-recombination epoch, leading to phase separation

Phase transition - dynamics

- Bubbles begin nucleating at some post-recombination epoch, leading to phase separation
- Early vacuum energy ρ_v swept up by the relativistically expanding bubbles, drops to its present value $\rho_\Lambda \approx 4 \text{ keV/cm}^3$ in the broken phase

Phase transition - dynamics

- Bubbles begin nucleating at some post-recombination epoch, leading to phase separation
- Early vacuum energy ρ_v swept up by the relativistically expanding bubbles, drops to its present value $\rho_\Lambda \approx 4 \text{ keV/cm}^3$ in the broken phase
- Expansion stops when adjacent bubble walls collide and disintegrate via emission of relativistic waves

Phase transition - dynamics

- Bubbles begin nucleating at some post-recombination epoch, leading to phase separation
- Early vacuum energy ρ_v swept up by the relativistically expanding bubbles, drops to its present value $\rho_\Lambda \approx 4 \text{ keV/cm}^3$ in the broken phase
- Expansion stops when adjacent bubble walls collide and disintegrate via emission of relativistic waves
- Fluctuation region quickly fills up with radiation, causing gravitational binding if certain conditions are met

Phase transition - dynamics

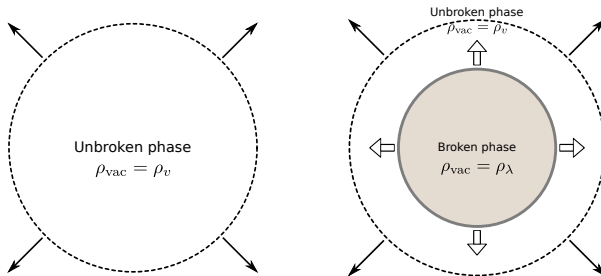


Figure: The figure on the left shows a comoving sphere expanding with the Hubble flow prior to the phase transition. In the figure on the right, a bubble of the broken phase nucleates at the center of the sphere and expands relativistically, sweeping up most of the early vacuum energy onto its boundary. The comoving sphere, meanwhile, continues to grow.

Phase transition - dynamics

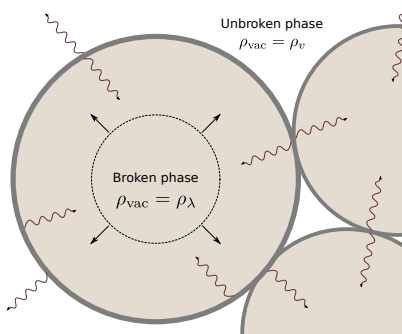


Figure: The relativistically expanding bubble eventually crosses the comoving sphere and collides with an adjacent bubble, radiating away the swept up energy in the form of unknown relativistic particles.

Binding of comoving shells

- Dynamics effectively described using Birkhoff's theorem

Binding of comoving shells

- Dynamics effectively described using Birkhoff's theorem
 - Statement of energy conservation

Binding of comoving shells

- Dynamics effectively described using Birkhoff's theorem
 - Statement of energy conservation

- Bubble-wall crossing: potential energy of comoving shell becomes less negative

Binding of comoving shells

- Dynamics effectively described using Birkhoff's theorem
 - Statement of energy conservation
- Bubble-wall crossing: potential energy of comoving shell becomes less negative
 - Comoving shell becomes temporarily unbound

Binding of comoving shells

- Bubble walls collide and disintegrate, radiation fills up the comoving region again, restoring the potential energy

Binding of comoving shells

- Bubble walls collide and disintegrate, radiation fills up the comoving region again, restoring the potential energy
- But comoving sphere has grown bigger in this time, so more potential energy restored than lost.

Binding of comoving shells

- Bubble walls collide and disintegrate, radiation fills up the comoving region again, restoring the potential energy
- But comoving sphere has grown bigger in this time, so more potential energy restored than lost.
- Total energy of system now negative: can lead to binding

Halting of the expansion

- At the end of this process, the equation of motion for the comoving shell under consideration is given by

$$\dot{a}^2(t; r) = \frac{8\pi G}{3} \left[\frac{\rho_{NR,c}}{a^3(t; r)} + \frac{\rho_{R,c}}{a^4(t)} + (\rho_v - \rho_\Lambda) \frac{a^4(t_f)}{a^4(t)} + \rho_\Lambda \right] a^2(t; r) + \frac{8\pi G}{3} (\rho_v - \rho_\Lambda) (a_c^2(r) - a^2(t_f))$$

Halting of the expansion

- At the end of this process, the equation of motion for the comoving shell under consideration is given by

$$\dot{a}^2(t; r) = \frac{8\pi G}{3} \left[\frac{\rho_{NR,c}}{a^3(t; r)} + \frac{\rho_{R,c}}{a^4(t)} + (\rho_v - \rho_\Lambda) \frac{a^4(t_f)}{a^4(t)} + \rho_\Lambda \right] a^2(t; r) + \frac{8\pi G}{3} (\rho_v - \rho_\Lambda) (a_c^2(r) - a^2(t_f))$$

- Shell of comoving radius r halts and begins to re-collapse when $\dot{a} = 0$, call this the “halting time”

Halting of the expansion

- At the end of this process, the equation of motion for the comoving shell under consideration is given by

$$\dot{a}^2(t; r) = \frac{8\pi G}{3} \left[\frac{\rho_{NR,c}}{a^3(t; r)} + \frac{\rho_{R,c}}{a^4(t)} + (\rho_v - \rho_\Lambda) \frac{a^4(t_f)}{a^4(t)} + \rho_\Lambda \right] a^2(t; r) + \frac{8\pi G}{3} (\rho_v - \rho_\Lambda) (a_c^2(r) - a^2(t_f))$$

- Shell of comoving radius r halts and begins to re-collapse when $\dot{a} = 0$, call this the “halting time”
- Representative timescale for formation of overdense regions

The energetics of halting

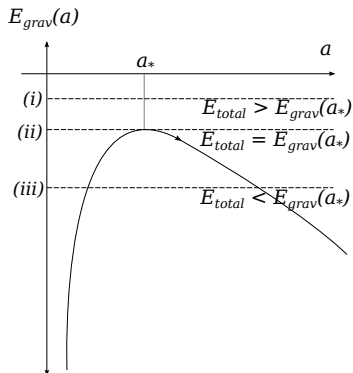


Figure: For halting to be accomplished, the kinetic energy has to drop to zero, which can only happen if the total energy is less than or equal to the maximum of the potential energy curve (cases (ii) and (iii)).

Conditions for binding/halting

- Early vacuum energy density ρ_v has to be several orders of magnitude higher than the current ρ_Λ

Conditions for binding/halting

- Early vacuum energy density ρ_v has to be several orders of magnitude higher than the current ρ_Λ
- Halting times are $\lesssim 1$ Gyr

Conditions for binding/halting

- Early vacuum energy density ρ_v has to be several orders of magnitude higher than the current ρ_Λ
- Halting times are $\lesssim 1$ Gyr
- Parameter space of critical temperature and early vacuum energy density

Conditions for binding/halting

- Early vacuum energy density ρ_v has to be several orders of magnitude higher than the current ρ_Λ
- Halting times are $\lesssim 1$ Gyr
- Parameter space of critical temperature and early vacuum energy density
- Halting times for different comoving radii at each point in parameter space

Fluctuation scale

- Typical ratio of transition width to Hubble time given by [5]

$$\delta \approx [4B_1 \ln(m_P/T_c)]^{-1}$$

Fluctuation scale

- Typical ratio of transition width to Hubble time given by [5]

$$\delta \approx [4B_1 \ln(m_P/T_c)]^{-1}$$

- $\delta \sim 1/300B_1$ for our range of critical temperatures
($B_1 \gtrsim \mathcal{O}(1)$)

Fluctuation scale

- Typical ratio of transition width to Hubble time given by [5]

$$\delta \approx [4B_1 \ln(m_P/T_c)]^{-1}$$

- $\delta \sim 1/300B_1$ for our range of critical temperatures
($B_1 \gtrsim \mathcal{O}(1)$)
- Nucleation scale given by δH_c^{-1}

Halting times across parameter space

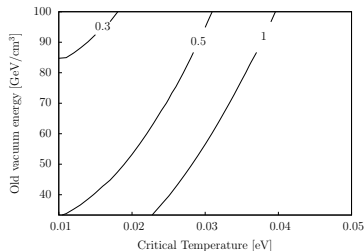
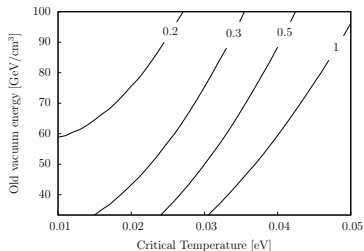


Figure: Figures showing contours of halting times across a parameter space spanned by critical temperature and early vacuum energy density. Ratios of coordinate radii of the chosen comoving shells to the typical nucleation scale are 10% and 50% respectively

Mass scale of fluctuations

- Mass scale of fluctuation region $M_f \approx \frac{4}{3}\pi(\delta H_c^{-1})^3 \rho_{NR,c}$

Mass scale of fluctuations

- Mass scale of fluctuation region $M_f \approx \frac{4}{3}\pi(\delta H_c^{-1})^3 \rho_{NR,c}$
- $M_f \sim 5 \times 10^8 M_\odot$ to $2 \times 10^{11} M_\odot$ across the parameter space

Mass scale of fluctuations

- Mass scale of fluctuation region $M_f \approx \frac{4}{3}\pi(\delta H_c^{-1})^3 \rho_{NR,c}$
- $M_f \sim 5 \times 10^8 M_\odot$ to $2 \times 10^{11} M_\odot$ across the parameter space
- Coarse upper limit. Mass scale associated with comoving region somewhat smaller $M \approx \frac{4}{3}\pi r^3 \rho_{NR,c}$

Mass scale of comoving regions

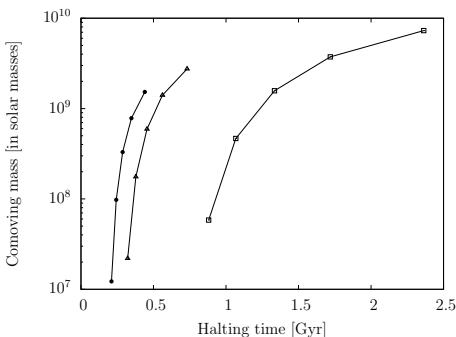


Figure: Mass scales corresponding to different halting times for specific parameter values. The three curves correspond to a fixed critical temperature of 0.03 eV and early vacuum energy densities of (from R to L) 33.3, 66.7 and 100 GeV/cm³ respectively

Outline

- 1 Big Black Holes and Late phase transitions
- 2 Sweeping up vacuum energy, à la Wasserman
- 3 Constraints**
- 4 Conclusion

Vacuum contribution to closure density at recombination

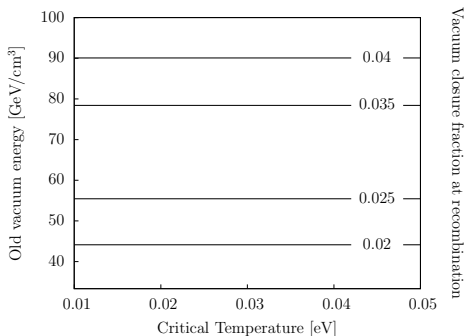


Figure: Contours of closure fraction of early vacuum energy density at recombination, across a parameter space spanned by critical temperature and early vacuum energy density. The expected lack of dependence on critical temperature may be noted.

Closure fraction of leftover radiation at current epoch

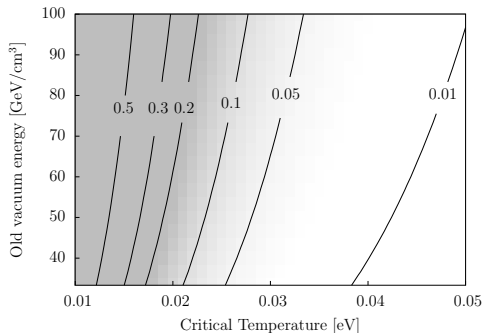


Figure: Contours of closure fraction at the current epoch, of the leftover radiation from the transition. Plotted against a parameter space spanned by critical temperature and early vacuum energy density.

Effect on Hubble parameter at current epoch

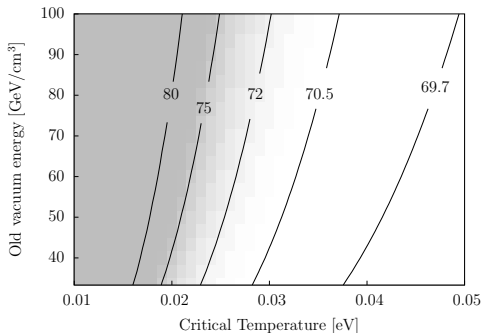


Figure: Contours of Hubble parameter at the current epoch, plotted against critical temperature and early vacuum energy density.

Imprint on the CMB

- Perturbations in the CMB due to these density fluctuations given by (Sachs-Wolfe effect)

$$\frac{\Delta T}{T} \sim \frac{GM_f}{R_f} = \frac{4\pi G}{3} \rho_{NR,c} R_f^2$$

Imprint on the CMB

- Perturbations in the CMB due to these density fluctuations given by (Sachs-Wolfe effect)

$$\frac{\Delta T}{T} \sim \frac{GM_f}{R_f} = \frac{4\pi G}{3} \rho_{NR,c} R_f^2$$

- For our range of critical temperatures

$$\frac{\Delta T}{T} \sim \frac{\rho_{NR,c}}{2\rho_c} \left[\frac{1}{300B_1} \right]^2$$

Imprint on the CMB

- Perturbations in the CMB due to these density fluctuations given by (Sachs-Wolfe effect)

$$\frac{\Delta T}{T} \sim \frac{GM_f}{R_f} = \frac{4\pi G}{3} \rho_{NR,c} R_f^2$$

- For our range of critical temperatures

$$\frac{\Delta T}{T} \sim \frac{\rho_{NR,c}}{2\rho_c} \left[\frac{1}{300B_1} \right]^2$$

- Safely within observed anisotropy bounds of ~ 1 part in 10^5

Other possible probes

- 21 cm observations

Other possible probes

- 21 cm observations
- Neutrino physics

Other possible probes

- 21 cm observations
- Neutrino physics
 - Range for T_c reminiscent of neutrino mass

Other possible probes

- 21 cm observations
- Neutrino physics
 - Range for T_c reminiscent of neutrino mass
 - Early vacuum energy $\rightarrow \nu\bar{\nu}$ (or $\nu_s\bar{\nu}_s$)

Other possible probes

- 21 cm observations
- Neutrino physics
 - Range for T_c reminiscent of neutrino mass
 - Early vacuum energy $\rightarrow \nu\bar{\nu}$ (or $\nu_s\bar{\nu}_s$)
 - Sum of light neutrino masses

Other possible probes

- 21 cm observations
- Neutrino physics
 - Range for T_c reminiscent of neutrino mass
 - Early vacuum energy $\rightarrow \nu\bar{\nu}$ (or $\nu_s\bar{\nu}_s$)
 - Sum of light neutrino masses
 - Evading eV-scale sterile neutrinos at recombination

Other possible probes

- 21 cm observations
- Neutrino physics
 - Range for T_c reminiscent of neutrino mass
 - Early vacuum energy $\rightarrow \nu\bar{\nu}$ (or $\nu_s\bar{\nu}_s$)
 - Sum of light neutrino masses
 - Evading eV-scale sterile neutrinos at recombination
 - Oscillations built-in at late times?

Other possible probes

- 21 cm observations
- Neutrino physics
 - Range for T_c reminiscent of neutrino mass
 - Early vacuum energy $\rightarrow \nu\bar{\nu}$ (or $\nu_s\bar{\nu}_s$)
 - Sum of light neutrino masses
 - Evading eV-scale sterile neutrinos at recombination
 - Oscillations built-in at late times?
 - Enhanced ν - ν interaction - dark matter models

Other possible probes

- 21 cm observations
- Neutrino physics
 - Range for T_c reminiscent of neutrino mass
 - Early vacuum energy $\rightarrow \nu\bar{\nu}$ (or $\nu_s\bar{\nu}_s$)
 - Sum of light neutrino masses
 - Evading eV-scale sterile neutrinos at recombination
 - Oscillations built-in at late times?
 - Enhanced ν - ν interaction - dark matter models
- Gravitational radiation probes?

Outline

- 1 Big Black Holes and Late phase transitions
- 2 Sweeping up vacuum energy, à la Wasserman
- 3 Constraints
- 4 Conclusion

Summary

- Pathway for formation of locally overdense regions on the scale of 10^6 – $10^9 M_{\odot}$ over cosmologically relevant timescales

Summary

- Pathway for formation of locally overdense regions on the scale of 10^6 – $10^9 M_{\odot}$ over cosmologically relevant timescales
- Possible solution to a long-standing problem in cosmology, i.e. formation of Big Black holes in the early universe

Summary

- Pathway for formation of locally overdense regions on the scale of 10^6 – $10^9 M_{\odot}$ over cosmologically relevant timescales
- Possible solution to a long-standing problem in cosmology, i.e. formation of Big Black holes in the early universe
- Different ways to associate microphysics with the transition, but many of the outcomes largely independent

Summary

- Pathway for formation of locally overdense regions on the scale of 10^6 – $10^9 M_{\odot}$ over cosmologically relevant timescales
- Possible solution to a long-standing problem in cosmology, i.e. formation of Big Black holes in the early universe
- Different ways to associate microphysics with the transition, but many of the outcomes largely independent
- \exists regions of parameter space that are not excluded by current cosmological constraints